Baeyer–Villiger oxidation of cyclic ketones using Fe containing MCM-48 cubic mesoporous materials

Hariharaputhiran Subramanian, Elizabeth G. Nettleton, Sridhar Budhi, Ranjit T. Koodali*

Department of Chemistry, University of South Dakota, 414 E. Clark Street, Vermillion, SD 57069, United States

ABSTRACT

Iron containing cubic mesoporous MCM-48 materials were prepared by a modified Stöber synthesis method. These materials were characterized by powder X-ray diffraction (XRD), nitrogen isotherms, diffuse-reflectance UV–Vis spectroscopy, and electron microscopy. These materials exhibited high catalytic activity towards the Baeyer–Villiger oxidation of cyclic ketones using benzaldehyde and molecular oxygen. The Fe-MCM-48 mesoporous materials showed excellent recyclability and the integrity of the cubic phase was preserved after the catalytic activity.

© 2010 Elsevier B.V. All rights reserved.

1. Introduction

Ordered mesoporous materials like MCM-41 [1], MCM-48 [1], and SBAs [2] etc. have been the subject of intensive research in the field of heterogeneous catalysis owing to their high surface area, uniform pores and relatively high thermal stability. These materials containing various transition metals [3,4] and its complexes [5,6] have been used as heterogeneous catalysts for several organic transformations [3–8]. Among the M41S series, the cubic form, MCM-48 is thought to be an important candidate for catalytic applications because of its interwoven and continuous 3-dimensional pore system that favors mass-transfer kinetics compared to the uni-dimensional pores that exist in the hexagonal form, MCM-41.

Baeyer–Villiger oxidation which was first reported in 1899 has wide synthetic utility [9]. It is used to convert readily available ketones to esters or lactones. Although several homogeneous catalytic systems have been reported there is an increased demand for heterogeneous catalytic systems due to the ease of separation and the prospect of easily reusing the catalyst for subsequent catalytic reactions [10,11].

Mukaiyama and co-workers reported the oxidation of aldehydes in the presence of oxygen using of Ni based catalysts [12]. In the year 1992, Murahashi et al. reported the heterogeneously catalyzed Baeyer–Villiger oxidation of ketones using aldehyde/O_2 as the oxidizing system by Fe_2O_3 based catalytic systems [13].

Since then several heterogeneous catalytic systems based on zeolites [14,15], hydrotalcites [16–19], microporous molecular sieves, MAlPO-36 (M = Mn or Co) [20], titanosilicates, TS-1 [21], mesoporous MCM-41 [22,23], and MCM-48 [4] have been reported to catalyze the Baeyer–Villiger oxidation under a variety of conditions. The oxidations that have been examined are hydrogen peroxide, persulfuric acid, perbenzoic acid, *m*-chloroperbenzoic acid (*m*-CPBA), and combination of benzaldehyde and molecular oxygen as stated earlier. However, studies involving heterogeneous catalytic Baeyer–Villiger oxidation of cyclic ketones using molecular oxygen and benzaldehyde are limited [3,13,16,19,20,24,25]. To the best of our knowledge, there exists no report on the use of Fe-MCM-48 mesoporous materials for the Baeyer–Villiger oxidation of cyclic ketones using molecular oxygen and benzaldehyde (Mukaiyama oxidant system).

Among the ordered M41S family of materials, the cubic form, MCM-48 has not been explored in great detail for catalytic reactions mainly because of the special conditions required to form them [26]. Several synthetic recipes reported for the cubic MCM-48 phase are often tedious, time consuming (2 days to several weeks), and conducted under hydrothermal conditions. It is attractive to develop new synthetic recipes that make use of simple surfactant molecules at room temperature.

Recently, we reported our preliminary results concerning Fe-MCM-48 materials for the oxidation of several ketones [27]. In this full report, we report the successful synthesis of Fe-MCM-48 materials at room temperature and the Baeyer–Villiger oxidation of cyclic ketones by the Fe-MCM-48 catalysts using benzaldehyde and molecular oxygen and examine the various factors affecting

---

the catalytic activity. We chose iron as the active species because iron is among the most abundant elements, inexpensive and is not toxic, i.e. environment friendly [3,28]. Several cyclic ketones are easily converted to the corresponding lactone compounds under relatively mild conditions with high catalytic activity.

2. Experimental

2.1. Synthesis

Fe-MCM-48 was prepared using a modified Stöber's synthesis at room temperature [29,30]. In a typical synthesis 1.2 g of hexadecyltrimethylammonium bromide (CTABr) (Alfa Aesar) and the required amount (0.0085–1.20 g) of ferric nitrate nonahydrate (Alfa Aesar) was taken in a polypropylene bottle (150 mL). To this 50 mL of deionized water and 25 mL of ethanol (AAPER 200 proof) was added and stirred well until the dissolution of the metal precursor. To this solution, 6 mL of NH_3 (~25 wt.%, Fisher) was added followed by 1.8 mL of tetraethoxysilane (TEOS) (Aldrich). The resulting solution was stirred for 4 h at room temperature at a stirring rate of 300 rpm. The precipitate obtained was filtered, washed with deionized water extensively. The solid was dried at $80 \pm 10\,°C$ for overnight in static air. The dried powder was ground finely and calcined in static air at $550\,°C$ at a heating rate of $3\,°C/min$ to remove the surfactant molecules for 6 h.

2.2. Characterization

The powder X-ray diffraction studies of the calcined samples were performed on a Scintag Pad V X-ray diffractometer with DSMNT data acquisition and analysis software and a Rigaku Ultima IV system equipped with PDXL software. The diffractometer was operated at 40 kV and 40 mA and the low angle regions were scanned from $2°$ to $6°$ (2θ) with a step size of 0.02. N_2 adsorption–desorption studies were carried out at liquid N_2 temperature (77 K) on a NOVA 2200e series apparatus. The surface areas were calculated using the Brunauer–Emmett–Teller equation in the relative pressure range (P/P_0) of 0.05–0.30. The pore volume was determined from the amount of nitrogen adsorbed at the highest relative pressure of $P/P_0 \sim 0.99$. The pore diameter was calculated by applying the Barrett–Joyner–Halenda (BJH) equation to the desorption isotherm. The samples were degassed at $100\,°C$ for at least 1 h prior to the isotherm measurements. The diffuse-reflectance (DR) spectra of Fe-MCM-48 materials were recorded using a Cary 100 Bio UV–Vis spectrophotometer equipped with a Harrick DR praying mantis accessory. The baseline correction was done using Si-MCM-48 material and the DR spectra were recorded in the wavelength region, 190–700 nm. The Fe content in the calcined MCM-48 materials and the spent catalysts were obtained using atomic absorption spectrometry (AAS) using a Thermo Jarell Ash atomic absorption spectrophotometer. For AAS studies, 0.25 g of iron filings was exactly weighed, dissolved in 25 mL of concentrated HCl, and the solution was transferred quantitatively to a 500 mL standard flask and diluted using deionized water. The concentration of Fe^{3+} in the solution so obtained was 500 ppm. From the 500 ppm stock solution of Fe^{3+}, solutions containing known amounts of Fe^{3+} were prepared. These solutions were analyzed using atomic absorption spectrometry and a calibration graph was plotted. A small amount of the Fe-MCM-48 sample was exactly weighed and stirred overnight with concentrated HCl. The silica was carefully filtered, and the filtrate was quantitatively transferred to a standard flask and diluted to a known volume. These solutions were analyzed for Fe^{3+} using atomic absorption spectrometry. From the calibration plot obtained previously, the exact amount of Fe^{3+} in the sample was calculated.
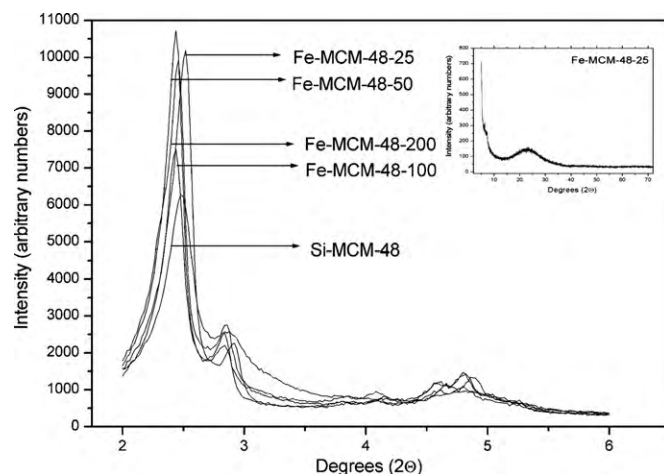

Fig. 1. Low angle powder XRD patterns of calcined Fe-MCM-48 mesoporous materials. The inset shows the high angle powder XRD patterns of Fe-MCM-48-25.

SEM experiments were conducted on a Zeiss Supra (40 VP FESEM) instrument. The SEM samples were prepared by spreading a small amount of the mesoporous sample on a double-coated tape fixed onto the aluminum specimen mount stub. The SEM images were typically obtained at the voltage of 4 keV and the condenser aperture setting was 20 μm and the sample working distance was 6 mm from the condenser aperture. The samples were generally not coated for the SEM studies. All the images were acquired with an in-lens detector. Transmission electron microscopy (TEM) images were recorded on a Hitachi H-7000 FA instrument (operating at 100 kV) and were obtained by sonicating an ethanolic solution containing Fe-MCM-48 before depositing them on carbon coated Cu TEM grids.

2.3. Catalytic experiments

The catalysts prepared were tested for Baeyer–Villiger oxidation of ketones. In a typical reaction benzaldehyde (6 mmol), nonane (internal standard, 1 mmol) were added to a three-necked flask fitted with a condenser and precharged with 0.1 g of the catalyst and 17 mL of 1,2-dichloroethane (DCE). The solution was refluxed at $50\,°C$ with continuous purging of O_2 at a flow rate of $10\,mL\,min^{-1}$. After 15 min, ketone (2 mmol) dissolved in 3 mL of DCE was added. After the completion of the reaction the catalyst was recovered, washed with acetone and dried in an air oven at $80 \pm 10\,°C$. The reaction mixture (after separation of the catalyst) was injected into the GC–MS (Shimadzu QP 5000) equipped with a silica column (J&W Scientific, 122-5532, DB-5ms equivalent to a (5% phenyl)methyl polysiloxane, 30 m × 0.25 mm). The conversion and yield of the product were determined using the internal standard (nonane) method. Further confirmation of the product(s) was made by Mass-Spectrometry. After the reaction, the catalyst was recovered, washed with acetone, dried in air, and used further for recycling experiments.

3. Results and discussion

3.1. XRD studies

A series of Fe-MCM-48 with varying Fe content were prepared using a modified Stöber synthesis [29,30]. The powder XRD patterns of the calcined Fe-MCM-48 (Fig. 1a) materials are consistent with those reported in the literature [31–33]. The XRD patterns indicate two peaks below $2\theta < 3.5°$ that are due to the (2 1 1) and (2 2 0) reflections. The presence of six additional peaks in the region

Table 1
Physico-chemical characterization of Fe-MCM-48 mesoporous materials.

Catalyst	Si/Fe ratio in the synthesis gel	Si/Fe ratio in calcined Fe-MCM-48	d_{211} (Å)	Unit cell parameter a_0 (Å)	Unit cell volume (Å)^3	Surface area (m^2/g)[a]	Pore volume (cm^3/g)[b]	Pore diameter (Å)[c]	Pore wall thickness (Å)[d]
Si-MCM-48	∞	0	35.56	87.10	660,797	1339	0.96	22.2	9.05
Fe-MCM-48-200	200	185	36.05	88.30	688,494	1979	1.2	22.0	7.84
Fe-MCM-48-100	100	116	36.32	88.96	704,002	1553	1.0	22.0	8.99
Fe-MCM-48-50	50	56	36.32	88.96	704,002	1545	1.1	26.1	8.41
Fe-MCM-48-25	25	30	35.23	86.30	642,669	1741	1.1	22.3	8.16

[a] Surface area determined by applying Brunauer–Emmett–Teller (BET) equation to a relative pressure (P/P_0) range of 0.05–0.30 in the adsorption isotherm.

[b] The pore volume (V) was calculated from the amount of nitrogen adsorbed at the highest relative pressure (P/P_0) of 0.99.

[c] The pore diameter was calculated from the Barrett–Joyner–Halenda (BJH) equation using the desorption isotherm.

[d] The thickness of the mesoporous materials were evaluated using the formula $t = [1 - (V_p\rho)/(1 + V_p\rho)](a_0/x_0)$, where V_p is the pore volume, ρ is the density of the pore wall (2.2 g/cm^3), a_0 is the unit cell parameter, and x_0 is a constant (3.0919).

of $2\theta = 3.5$–$6°$ are due to the (3 2 1), (4 0 0), (4 2 0), (3 3 2), (4 2 2) and (4 3 1) reflections in the *Ia3d* space group. This is an indication of the high quality of the cubic phase. From the X-ray diffractogram, we can observe that the highest intense peak due to d_{211} plane is shifted towards the lower angle region for the samples labeled Fe-MCM-48-200, 100 and 50 indicating an increase in the d_{211} value; in contrast for the sample labeled Fe-MCM-48-25, the highest peak appears slightly to the right of siliceous MCM-48 indicating a decrease in the unit cell parameter, (a_0). From the X-ray diffractogram, the d_{211} and the unit cell parameter (a_0) were calculated for Si-MCM-48 and Fe-MCM-48 materials using the relation $a_0 = d\sqrt{6}$ and these results are summarized in Table 1. The unit cell parameter (a_0) increases with increase in Fe content and then drops. The unit cell parameter (a_0) increased with increase in the Fe content and then leveled off when compared to Si-MCM-48. The increase in the unit cell dimension (entries 2 and 3) could be possibly attributed to the larger crystal radius of Fe^{3+} (0.63 Å) compared to Si^{4+} (0.40 Å) and/or the longer Fe–O bond distance ($\sim$2.0 Å) as compared to the Si–O distance (1.6 Å). Similar trends in the unit cell parameter have been reported by others [3,34,35]. Thus, the powder XRD results indicate the framework substitution of Si^{4+} ion in MCM-48 by Fe^{3+} at Si/Fe ratios of 200, and 100. The powder XRD patterns were also examined in the high angle region for all the samples. The inset in Fig. 1 shows the powder XRD patterns in the 2θ range of 2–74° for Fe-MCM-48-25. All the Fe-MCM-48 samples show similar patterns as that of Fe-MCM-48-25. The powder XRD patterns reveal a broad peak around $2\theta = 22°$ that is due to silica. No distinct peak due to the presence of iron oxide can be seen in any of the samples. This may be either due to the low amount of iron in the two samples, Fe-MCM-48-200 and Fe-MCM-48-100 and due to the high dispersion of iron in the samples containing relatively high amounts of iron, i.e. Fe-MCM-48-50 and Fe-MCM-48-25. The color of the Fe containing samples is a simple visual indicator of the existence of bulk iron oxide in these materials [3,36]. All the as-synthesized Fe-MCM-48 samples were white in color, whereas the calcined materials exhibited slight color depending on the Fe content. The samples, Fe-MCM-48-200, and 100 were white in color suggesting that the iron was in the framework whereas the samples labeled Fe-MCM-48-50, and 25 were off-white in color indicating that some iron existed outside the framework.

3.2. Diffuse-reflectance UV–Vis spectroscopy

Fig. 2 shows the diffuse-reflectance (DR) UV–Vis absorption spectra of Fe-MCM-48 (Si/Fe = 200, 100, 50, and 25). Two distinct peaks one centered near 240 nm and the other around 295 nm are seen in the spectrum. The peaks at 240 nm and 295 nm are due to isolated Fe^{3+} species in tetrahedral coordination and the origin of the band may be attributed to $d\pi$–$p\pi$ charge-transfer between Fe^{3+} and oxygen anions [32,37]. There is an additional broad peak in the region 320–350 nm for Fe-MCM-48 (Si/Fe = 50, 25) that may

be attributed to oligomeric iron species $(FeO)_n$ [36]. Thus, the DR spectra indicate that the Fe^{3+} is present in tetrahedral positions at ratios of Si/Fe = 200 and 100 whereas some oligomeric iron species is present in the samples prepared with Si/Fe ratios of 50 and 25.

3.3. Atomic absorption spectrophotometric studies

The Fe content in the calcined MCM-48 materials was calculated using atomic absorption spectrometry (AAS). Table 1 lists the Si/Fe ratios in the wet gel and the calcined material. The Fe content in the calcined materials is almost similar to the expected Fe content in the wet gel, indicating very good incorporation of most Fe^{3+} into the mesoporous MCM-48 material by the direct synthesis method at room temperature.

3.4. N$_2$ adsorption studies

Table 1 also contains a summary of the textural properties (surface areas, pore volumes, and pore sizes) and the pore wall thickness of Fe-MCM-48 materials. These materials are characterized by very high specific surface areas (1300–2000 m^2/g) and large pore volumes (0.9–1.2 cm^3/g). The pore diameters of these materials are fairly uniform around, 22 Å, except for the Fe-MCM-48-50 material. The pore wall thickness of the MCM-48 materials varies very little with Fe content. Fig. 3 shows the nitrogen adsorption isotherm of Fe-MCM-48 materials with Si/Fe ratios of 200, 100, and 25. The isotherm of the sample, Fe-MCM-48-50 is not shown for the sake of clarity. A typical reversible type IV isotherm with H1 hysteresis loop is observed for all the materials. At relative pres-
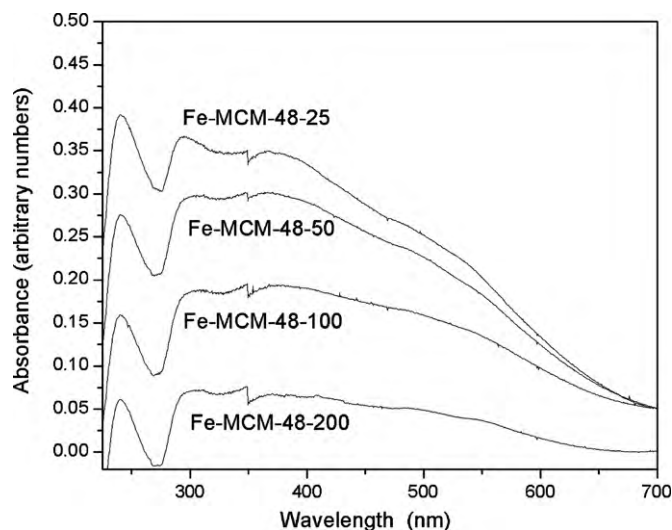

Fig. 2. Diffuse-reflectance spectra of calcined Fe-MCM-48 mesoporous materials.
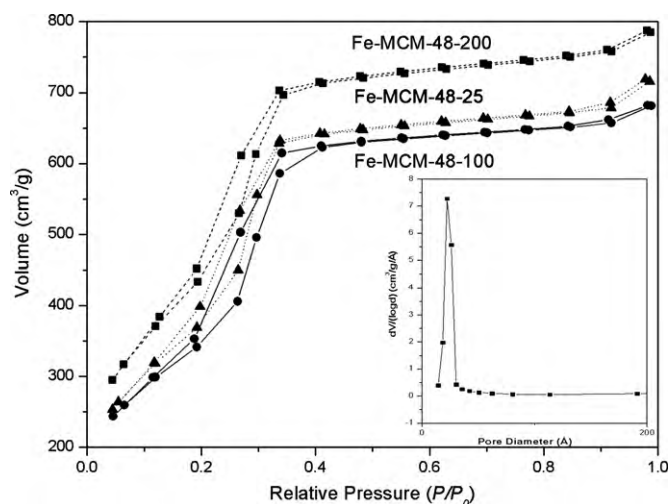
Fig. 3. Nitrogen adsorption isotherms of Fe-MCM-48 mesoporous materials. The inset shows the pore size distribution in Fe-MCM-48-25.

sures, P/P_0 between 0.2 and 0.4, a sharp inflection due to capillary condensation within the mesopores is observed, which is characteristic of ordered mesoporous materials such as MCM-48. Fig. 3b shows that the pore size distribution of Fe-MCM-48-25 material is highly uniform.

3.5. Electron microscopic studies

Scanning electron microscopic image of a representative Fe-MCM-48 material is shown in Fig. 4. The SEM image indicates that the particles are fairly spherical with minimal aggregation.

Transmission electron microscopic studies were also performed in order to elucidate the nature of the pores. The TEM image (recorded along the cubic [1 1 0] plane, Fig. 5) for a representative Fe-MCM-48 material indicates that the pores are regular and the pore size is estimated to be slightly over 2 nm consistent with Nitrogen sorption and powder X-ray experiments. The linear regular array of mesopores and walls is consistent with previous reports of the cubic MCM-48 phase [29].

3.6. Baeyer–Villiger oxidation of ketones

The Fe-MCM-48 materials were evaluated for the Baeyer–Villiger oxidation of several cyclic ketones. Our preliminary experiments were carried out with 2-adamantanone as the sub-
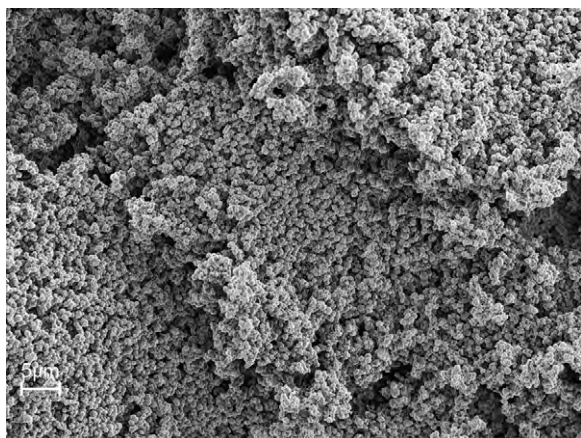
Fig. 4. Scanning electron microscopic image of Fe-MCM-48-200.
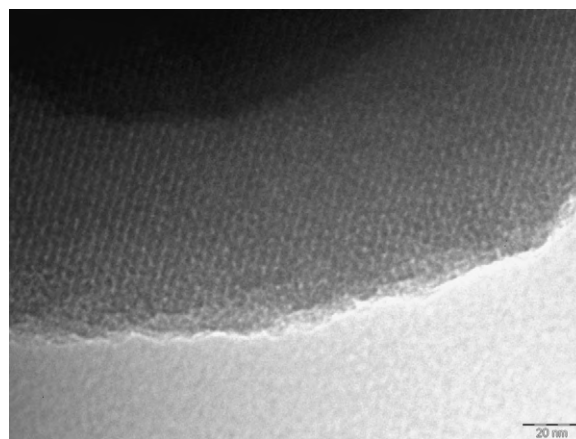
Fig. 5. Transmission electron microscopic image of Fe-MCM-48-200 recorded along the cubic [1 1 0] plane.

strate. The results of Baeyer–Villiger oxidation of 2-adamantanone using MCM-48 based catalysts in 1,2-dichloroethane (DCE) as the solvent are shown in Table 2. In the presence of Si-MCM-48 the reaction hardly proceeded (entry 1) after 2 h at 50 °C. Impressive conversions and yields are obtained with the addition of very little amount of Fe into the framework, i.e. as low as 0.54 wt.% (entry 2). With an increase in the amount of the catalytically active site, i.e. Fe^{3+} content, (0.86 wt.%), there was an increase in the conversion and yield due to a presence of more Fe^{3+} in the framework position, that does not leach under the experimental conditions used in this study. Addition of more Fe^{3+} in the synthesis gel however leads to the formation of also extra-framework Fe^{3+} in the case of Fe-MCM-48-50 and Fe-MCM-48-25. Thus, in the samples, Fe-MCM-48-50 and 25, the supernatant solution was found to be colored at the end of the reaction. This indicates the presence of Fe^{3+} that has leached out from the MCM-48 material. AAS results confirm the presence of Fe^{3+}. In these two samples, powder XRD, and DR spectra suggest the presence of extra-framework Fe^{3+} species and the results obtained from the catalytic experiments suggest that the extra-framework Fe^{3+} are not stable in the solvent, 1,2-DCE employed in the reaction. In all the reactions, benzoic acid was also detected as the by-product. No transesterification products were detected in any of the reactions. For comparison purposes, we also prepared V and Ti containing MCM-48 materials at low ratios, i.e. Si/M = 200, where M = Ti or V. However, negligible or only trace amounts of the corresponding lactone were observed. In the case of the siliceous Si-MCM-48, and the V-MCM-48, trace amounts of benzoic acid were also detected as by-products. At the moment, we are unable to offer any explanation for the inactivity

Table 2
Baeyer–Villiger oxidation of 2-adamantanone using MCM-48 based catalysts.

Entry	Catalyst	Conversion (%)[a]	Yield (%)[a]
1	Si-MCM-48	11	9.5
2	Fe-MCM-48-200	89	80
3	Fe-MCM-48-100	95	95
4	Fe-MCM-48-50	95[b]	95[b]
5	Fe-MCM-48-25	95[b]	95[b]
6	None	14[c]	<1[c]
7	V-MCM-48-200	10	9.5
8	Ti-MCM-48-200	Trace	Trace
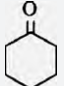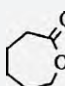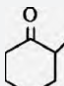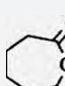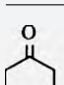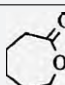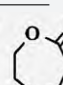
Reaction conditions: 2-adamantanone (2 mmol), benzaldehyde (6 mmol), nonane (0.2 mL), catalyst (0.1 g), and 1,2-dichloroethane (20 mL). The system was purged continuously with O_2 (10 mL min^{-1}) at 50 ± 5 °C for 2 h.
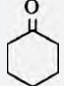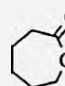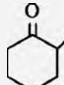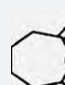[a] Calculated by GC–MS based on the internal standard (nonane).
[b] Leaching of Fe observed.
[c] The reaction was carried out in the absence of Fe-MCM-48 catalyst.

Table 3
Baeyer–Villiger oxidation of ketones using cubic mesoporous Fe-MCM-48-200 (0.54 wt.%) catalyst.

Entry	Ketone	Product	Conversion (%)[a]	Yield (%)[a]
1			92	62
2			83	80
3			72	38[b]
4			89	81
5			10	Trace

Reaction conditions: substrate (2 mmol), benzaldehyde (6 mmol), nonane (0.2 mL), catalyst (0.1 g), and 1,2-dichloroethane (20 mL). The system was purged continuously with O_2 (10 mL min^{-1}) at $50 \pm 5\,°C$ for 2 h.
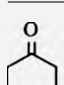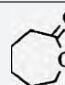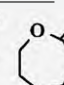
[a] Calculated by GC–MS based on the internal standard (nonane).
[b] The product selectivity was 1:1.

Table 4
Baeyer–Villiger oxidation of ketones in the absence of any catalyst.

Entry	Ketone	Product	Conversion (%)[a]	Yield (%)[a]
1			24	20
2			34	5
3			25	<1
4			14	1
5			0	0

Reaction conditions: substrate (2 mmol), benzaldehyde (6 mmol), nonane (0.2 mL), 1,2-dichloroethane (20 mL). The system was purged continuously with O_2 (10 mL min^{-1}) at $50 \pm 5\,°C$ for 2 h.
Note: Benzoic acid was observed in all these reactions.

[a] Calculated by GC–MS based on the internal standard (nonane).
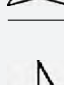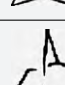
of the Ti and V containing MCM-48 catalysts. The focus of this paper is on the Fe-MCM-48 materials and hence we explored the catalytic activity of these materials in detail. In the absence of any catalyst, the conversion of 2-adamantanone was found to be 14%, whereas the yield (selectivity) of the corresponding lactone was negligible, i.e. <1% due to the possible formation of polymers. For comparison purposes, we also prepared Fe-MCM-48-200 by an impregnation method. First, Si-MCM-48 was prepared and then the required amount of $Fe(NO_3)_3 \cdot 9H_2O$ was impregnated on the mesoporous support. Although the activity of this sample was comparable to that of the Fe-MCM-48-200 prepared by direct synthesis, AAS studies indicate that almost all the iron had leached out of the mesoporous support after the reaction and any catalytic activity exhibited is due to the homogeneous reaction of $Fe(NO_3)_3$ dissolved in DCE and the substrate.

The catalytic activities of Fe-MCM-48 towards Baeyer–Villiger oxidation of other cyclic ketones were also explored. Typical catalytic performances using the Fe-MCM-48-200 (0.54 wt.% Fe) is shown in Table 3. Almost all the cyclic ketones are converted to corresponding lactones with high selectivity except norcamphor (entry 5) which exhibited low conversions and yields. The low conversion and yield is probably due to substrate reactivity effects. The catalytic activity of Fe-MCM-48-100 (0.86 wt.% Fe) was found to be higher compared to Fe-MCM-48-200 (0.54 wt.% Fe) for the oxidation of all the ketones examined in the study, barring norcamphor which showed very little activity. The higher activity may be attributed to the presence of higher Fe^{3+} amounts in these materials. Although, the samples Fe-MCM-48-50 and 25 contain higher amounts of Fe^{3+} compared to Fe-MCM-48-200 and 100, their catalytic activities were not evaluated since leaching was observed when 2-adamantanone was used as the substrate when these catalysts were employed.

The oxidation of 2-methylcylcohexanone leads to the formation of only 7-methyloxepan-2-one as indicated in Table 3 (entry 2). The BVO reaction mechanism is a two-step process [38]. In the first step, the peroxy acid generated in situ undergoes a reversible nucleophilic attack on the carbonyl group of the ketone. This leads to the formation of a tetrahedral intermediate, the Criegee adduct. In the second step, an irreversible migration of one of the two substituents and a simultaneous cleavage of the O–O bond in a concerted manner leads to the formation of benzoic acid and the lactone (in our case). It is established that the rearrangement is regioselective. The group that is best able to stabilize the developing positive charge on the carbonyl carbon is more prone to migration. In the oxidation of 2-methylcyclohexanone, the transition state leading to the formation of 7-methyloxepan-2-one is more stable compared to the one that could form 3-methyloxepan-2-one and hence only one product, i.e. 7-methyloxepan-2-one is formed. However, the oxidation of 3-methylcyclohexanone leads to the formation of both 6-methyloxepan-2-one and 4-methyloxepan-2-one (Table 3, entry 3) with equal selectivity. This is because the migratory aptitude of the two groups is similar and hence we obtain equal amounts of the two products, i.e. 6-methyloxepan-2-one and 4-methyloxepan-2-one. The yield of the product(s) is different from the conversion and this may be due to the formation of polymeric species as postulated by Kawabata et al. or due to the formation of hydroxyacids [3,38].

In the absence of any catalyst, no lactones were detected; however benzoic acid was always detected, formed by the reaction of benzaldehyde and molecular oxygen. The conversions were generally low and the yields negligible in the absence of the catalysts. The results are shown in Table 4.

The activity of Fe-MCM-48 catalysts in the present investigation are superior to the activity of MCM-41 mesoporous materials reported viz., Fe-MCM-41 [3] (61% yield in 4 h) under identical experimental conditions. This may be attributed to the interwoven three-dimensional pore system present in the MCM-48 materials which favors mass-transfer kinetics for the diffusion of large and bulky molecules such as 2-adamantanone. Furthermore, the presence of Fe^{3+} in tetrahedrally coordinated sites seems to be a necessity for the stability of Fe^{3+} in the mesopore matrix.

Table 5
Baeyer–Villiger oxidation of cyclohexanone using different oxidizing agents by Fe-MCM-48-200 (0.54 wt.% Fe) catalyst.

Entry	Oxidant	Conversion (%)[a]
1	Benzaldehyde/O_2[b]	98
2	m-CPBA[c]	98
3	H_2O_2[c]	0
4	O_2[d]	0
5	$tert$-Butyl hydrogen peroxide[b]	0
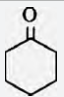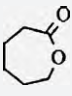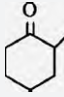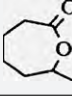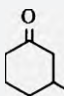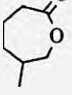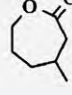
[a] Calculated by GC–MS based on the internal standard (nonane).
[b] Cyclohexanone (2 mmol), benzaldehyde (6 mmol), nonane (0.2 mL), catalyst (0.1 g), 1,2-dichloroethane (20 mL). The system was purged continuously with O_2 at ~50 °C for 2 h.
[c] Cyclohexanone (2 mmol), oxidant (3 mmol), nonane (0.2 mL), catalyst (0.1 g), 1,2-dichloroethane (20 mL). The mixture was refluxed at 50 °C.
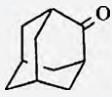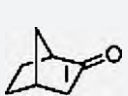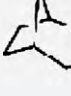[d] Cyclohexanone (2 mmol), nonane (0.2 mL), catalyst (0.1 g), 1,2-dichloroethane (20 mL). The system was purged continuously with O_2 (10 mL min^{-1}) at 50 ± 5 °C for 2 h.

In the current investigation we also explored the use of other oxidizing agents for the Baeyer–Villiger oxidation. Table 5 shows the results of various oxidizing agents on the Baeyer–Villiger oxidation of cyclohexanone. Among the oxidizing agents used, O_2 (alone), H_2O_2 and TBHP were found to be inefficient under the given conditions and m-CPBA was also found to be a good oxidizing agent. We explored the catalytic activity using m-CPBA as the oxidant and the results are shown in Table 6. Very high conversions and yields were obtained using m-CPBA. The activity of the norcamphor was found to be low, 50% yield was obtained only after 17 h of the reaction.

3.7. Recycling studies

Table 7 shows the results of reusability of the solid catalyst. The use of a solid catalyst affords simple workup over conventional homogeneous catalysts. After the Baeyer–Villiger reaction, the Fe-MCM-48-200 catalyst was easily recovered by simple filtration and reused for further catalytic reactions. From Table 7 it can be seen that the Fe-MCM-48-200 catalyst could be used for at least

Table 6
Baeyer–Villiger oxidation of various ketones using Fe-MCM-48-200 (0.54 wt.%) mesoporous materials and m-CPBA as the oxidant.

Entry	Ketone	Product	Time (h)	Conversion (%)[a]
1			5	98
2			5	98
3			5	100[b]
4			5	86
5			17	50

Reaction conditions: substrate (2 mmol), m-CPBA (2 mmol), nonane (0.2 mL), catalyst (0.1 g), and 1,2-dichloroethane (20 mL). The mixture was refluxed at 50 ± 5 °C.
[a] Calculated by GC–MS using the internal standard (nonane).
[b] 100% conversion was reached in 3 h and then remained essentially constant.

Table 7
Recyclability of Fe-MCM-48-200 (0.54 wt.%) for the Baeyer–Villiger oxidation of 2-adamantanone.

Entry	Catalyst	Conversion (%)[a]	Yield (%)[a]
1	Si-MCM-48	11	9.5
2	Fe-MCM-48-200 (fresh)	89	80
3	Fe-MCM-48-200[b]	86	83
4	Fe-MCM-48-200[c]	89	81

Reaction conditions: 2-adamantanone (2 mmol), benzaldehyde (6 mmol), nonane (0.2 mL), catalyst (0.1 g), 1,2-dichloroethane (20 mL). The system was purged continuously with O_2 (10 mL min^{-1}) at 50 ± 5 °C for 2 h.
[a] Calculated by GC–MS using the internal standard (nonane).
[b] First recycled catalyst.
[c] Second recycled catalyst.

three cycles without any appreciable loss in its catalytic activity. The AAS analysis of the spent catalyst revealed that there was no leaching of Fe species into the solution. Also from the XRD pattern (not shown) of the spent catalyst, it can be inferred that the cubic mesophase had not collapsed. The UV–Vis DR spectrum of Fe-MCM-48-200 was recorded after recovering the catalyst and the results indicated that the spectra remain virtually unchanged after the BV-oxidation. The UV spectra of MCM-48-200 showed peaks near 240 nm and 295 nm while the spent catalyst showed peaks near 242 nm and 296 nm; however since both these spectra overlap considerably, the UV spectra of the spent catalyst is not shown for the sake of clarity.

Thus, a combination of catalytically active Fe^{3+} species in tetrahedral coordination and the continuous 3D pore system present in the MCM-48 materials are responsible for achieving high selectivity.

3.8. Reaction mechanism

Corma et al. [14] have postulated that the carbonyl group in the cyclic ketone was activated in the presence of the oxidant, H_2O_2. The reaction on Sn containing β zeolite and Sn exchanged hydrotalcites [39] was thought to proceed through a Criegee adduct of the activated ketone and the hydrogen peroxide. Kawabata et al. [3] suggested that the reaction proceeded via the coordination of carbonyl groups of ketone to Fe^{3+} as Lewis acid sites. We also believe that a similar mechanism is operative in our catalytic reaction. The catalytic experiments were performed by pre-charging the reactor with benzaldehyde and continuously purging with molecular oxygen and the substrate, i.e. ketone was added after 15 min. However, if the ketone was added initially along with benzaldehyde, there was an induction period for the formation of the lactone. This indicates that the reaction of benzaldehyde and molecular oxygen produces perbenzoic acid *in situ* and that it is necessary for the formation of the product(s). The tetrahedral Fe^{3+} Lewis acid sites in the MCM-48 material activates the substrate and the activated ketone molecules attacks the perbenzoic acid produced *in situ* to form a Criegee adduct [15,40]. The Criegee adduct undergoes protolysis, to afford the lactone and the by-product benzoic acid. Benzoic acid is formed in almost stoichiometric amounts, i.e. ~6 mmol corresponding to 1 equiv. of benzaldehyde used as the sacrificial oxidant.

4. Conclusion

We have developed a simple method for the preparation of Fe containing MCM-48 mesoporous materials at room temperature using a modified Stöber synthesis. Fe^{3+} can be incorporated up to 0.86 wt.% in the tetrahedral framework by the direct synthesis. The Fe-MCM-48 materials exhibited excellent activity for the Baeyer–Villiger oxidation of several cyclic ketones using molecu-

lar oxygen and benzaldehyde as the oxidants. The catalyst could be reused without any appreciable loss in activity and the structure of the cubic mesoporous materials were found to be intact after the catalytic reaction and no leaching was observed for the Fe-MCM-48 samples that had Fe in tetrahedral coordination.

References

[1] C.T. Kresge, M.E. Lenowicz, W.J. Roth, J.C. Vartuli, J.S. Beck, Nature 359 (1992) 710.
[2] A. Firouzi, D. Kumar, L.M. Bull, T. Besier, Q. Huo, S.A. Walker, J.A. Zasadzinski, C. Glinka, J. Nicol, D. Margolese, G.D. Stucky, B.F. Chmelka, Science 267 (1995) 1138.
[3] T. Kawabata, Y. Ohishi, S. Itsuki, N. Fujisaki, T. Shishido, K. Takaki, Q. Zhang, Y. Wang, K. Takehira, J. Mol. Catal. A 236 (2005) 99.
[4] D.H. Koo, M. Kim, S. Chang, Org. Lett. 7 (2005) 5015.
[5] C. Baleizao, B. Gigante, D. Das, M. Alvaro, H. Garcia, A. Corma, Chem. Commun. (2003) 1860.
[6] A. Adima, J.J.E. Moreau, M.W.C. Man, J. Mater. Chem. 7 (1997) 2331.
[7] B.M. Choudary, M.L. Kantam, B. Bharathi, P. Sreekanth, F. Figueras, J. Mol. Catal. A 159 (2000) 417.
[8] B.M. Choudary, N.S. Chowdari, M.L. Kantam, P.L. Santhi, Catal. Lett. 76 (2001) 213.
[9] A. Baeyer, V. Villiger, Ber. Dtsch. Chem. Ges. 32 (1899) 3625.
[10] A. Yoshida, M. Yoshimura, K. Uehara, S. Hikichi, N. Mizuno, Angew. Chem. Int. Ed. 45 (2006) 1956.
[11] A. Corma, Catal. Rev. Sci. Eng. 46 (2004) 369.
[12] T. Yamada, O. Rhode, T. Takai, T. Mukaiyama, Chem. Lett. (1991) 5.
[13] S.I. Murahashi, Y. Oda, T. Naota, Tetrahedron Lett. 33 (1992) 7757.
[14] A. Corma, L.T. Nemeth, M. Renz, S. Valencia, Nature 412 (2001) 423.
[15] M. Renz, T. Blasco, A. Corma, V. Fornes, R. Jensen, L. Nemeth, Chem. Eur. J. 8 (2002) 4708.
[16] K. Kaneda, S. Ueno, T. Imanaka, Chem. Commun. (1994) 797.
[17] K. Kaneda, Y. Yamashita, Tetrahedron Lett. 37 (1996) 4555.
[18] S. Ueno, E. Kohki, O. Akira, K. Kaneda, Appl. Surf. Sci. 121 (1997) 366.
[19] K. Kaneda, S. Ueno, T. Imanaka, J. Mol. Catal. A 102 (1995) 135.
[20] R. Raja, J.M. Thomas, G. Sankar, Chem. Commun. (1999) 525.
[21] A. Bhaumik, P. Kumar, R. Kumar, Catal. Lett. 40 (1996) 47.
[22] A. Corma, M.T. Navarro, M. Renz, J. Catal. 219 (2003) 242.
[23] A. Corma, M.T. Navarro, L.M. Nemeth, M. Renz, Chem. Commun. (2001) 2190.
[24] K. Kaneda, S. Ueno, T. Imanaka, E. Shimotsuma, Y. Nishiyama, Y. Ishii, J. Org. Chem. 59 (1994) 2915.
[25] K. Kaneda, S. Haruna, T. Imanaka, K. Kawamoto, Chem. Commun. (1990) 1467.
[26] M. Morey, A. Davidson, G.D. Stucky, J. Porous Mater. 5 (1998) 195.
[27] H. Subramanian, R.T. Koodali, React. Kinet. Catal. Lett. 95 (2008) 239.
[28] N.I. Sax, Dangerous Properties of Industrial Materials, Sixth ed., Van Nostrand Reinhold Company Inc., New York, 1984.
[29] K. Schumacher, C. du F. von Hohenesche, K.K. Unger, R. Ulrich, A. Du Chesne, U. Wiesner, H.W. Spiess, Adv. Mater. 11 (1999) 1194.
[30] B. Boote, H. Subramanian, K.T. Ranjit, Chem. Commun. (2007) 4543.
[31] W. Zhao, L. Kong, Y. Luo, Q. Li, Micropor. Mesopor. Mater. 100 (2007) 111.
[32] Y. Shao, L. Wang, J. Zhang, M. Anpo, J. Phys. Chem. B 109 (2005) 20835.
[33] B. Echchahed, A. Moen, D. Nicholson, L. Bonneviot, Chem. Mater. 9 (1997) 1716.
[34] A.B. Bourlineous, M.A. Karakassides, D. Petridis, J. Phys. Chem. 104 (2000) 4375.
[35] P. Selvam, S.E. Dapurkar, S.K. Badamali, M. Murugesan, H. Kuwano, Catal. Today 68 (2001) 69.
[36] P. Ratnasami, R. Kumar, Catal. Today 9 (1991) 329.
[37] P. Kustrowski, L. Chmielarz, J. Surman, E. Bidzinska, R. Dziembaj, P. Cool, E.F. Vansant, J. Phys. Chem. A 109 (2005) 9808.
[38] C. Jimenez-Sanchidrian, J.R. Ruiz, Tetrahedron 64 (2008) 2011.
[39] U.R. Pillai, E. Sahle-Demessie, J. Mol. Catal. 191 (2003) 93.
[40] A. Brunetta, G. Strukul, Eur. J. Inorg. Chem. (2004) 1030.